Letter

Online Sequential Fractionation Analysis of Arsenic Adsorbed onto Ferrihydrite by ICP-MS

Debo Wu, Shuiping Yang, Faliang Li, Tenggao Zhu, and Huanwen Chen*

Read Online

ACCESS | 📊 Metrics & More | 📖 Article Recommendations | 🆂🆕 Supporting Information

ABSTRACT: Fractionation information on arsenic (As) in complex samples, particularly solid samples, is of immense interest. Herein, selective extraction of various As species adsorbed onto ferrihydrite as the model substrate was online-adapted to inductively coupled plasma-mass spectrometry (ICP-MS) for sensitive detection. The As-adsorbed ferrihydrite sample was loaded into a homemade online sequential elution device using two commercially available micropipette tips, and then, each fraction of As including nonspecifically adsorbed, specifically adsorbed, iron oxide bonded, and residual species was successively extracted for ICP-MS detection, with H_2O, NH_4NO_3, $NH_4H_2PO_4$, ammonium oxalate, and HF as the eluents, respectively. While no water-soluble As was detected, the fraction of As bonded to iron oxide was detected as the dominant species (>80%), and the specifically adsorbed As and residual As also accounted for a substantial amount (10%). The method had a detection limit of 0.008 $\mu g/kg$ for As(III) and 0.013 $\mu g/kg$ for As(V), with merits such as extremely low sample consumption, high throughput, and minimized experimental manipulation, presenting an alternative strategy for sensitive fractionation analysis of As adsorbed onto solid substrates (e.g., iron oxides, etc.).
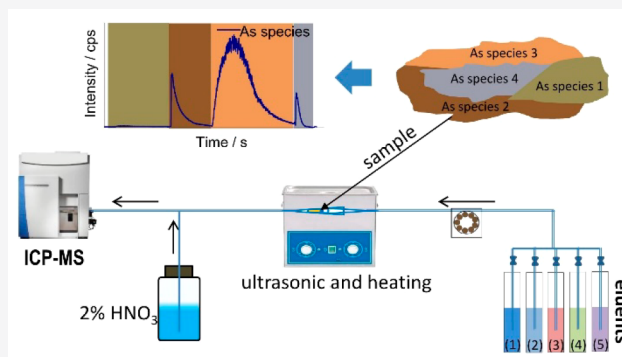
Iron oxides are naturally strong adsorbents for arsenic element. Thus, fractionation analysis of arsenic (As) on the surface of various iron-containing minerals plays a key role in revealing its toxicity, mobility, bioavailability, and transformation in a natural environment.[1,2] As could exist in different forms such as water-soluble, nonspecifically adsorbed, specifically adsorbed, iron oxide bonded, and residual species[3] on the surface of iron oxides. Unfortunately, determination of the total As concentrations in solid samples such as soils and sediments could not reveal any information regarding its chemical form and potential mobility. X-ray absorption spectroscopy (XAS) can provide detailed information on the speciation and coordination of As in soils; however, in many soils and sediments, As concentrations are too low for high-quality XAS measurements.[4,5] XRD allowed identification of As-bearing solid phases, but a high degree of crystallinity and a high As content as well are necessary.[6] Although X-ray photoelectron spectroscopy (XPS) was sometimes used to characterize the microstructure of As species on iron oxides,[7] the quantification information on trace levels of As species was hardly available.

On the other hand, conventional analytical methods normally involve tedious sample pretreatment procedures such as digestion, dilution, acidification, and preservation, especially for solid samples. Each step is time-consuming and may suffer from contamination or mass loss.[8] Offline sequential extraction process (SEP) is a sample pretreatment

technique for fractionation and extraction of heavy metals and other elements into different forms according to the association between heavy metals and soil components.[9,10] The Tessier method and BCR (Community Bureau of Reference protocol) methods are the most commonly used SEP methods.[9,10] However, As is a multispecies metalloid that mainly exists at a trace level as anions in the environment,[11,12] so the conventional SEP methods are not fully suitable for fractionation analysis of As.

Study of the associations between As and iron oxides provides chemical insights on the adsorption mechanism, environmental interaction,[13−15] and geochemical behaviors. Considering that the distribution of As in a natural environment is closely correlated with that of iron oxides, a novel method based on sequential online extraction of As species adsorbed onto ferrihydrite for sensitive detection by ICP-MS was developed. As illustrated in Figure 1, As-adsorbed ferrihydrite was loaded into a homemade online sequential elution device, which was coupled to ICP-MS, and various As
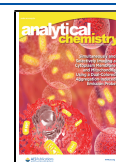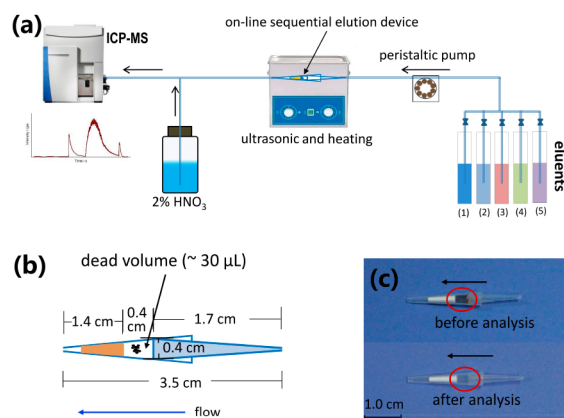
Figure 1. (a) Schematic of sequential online detection of As species adsorbed onto ferrihydrite by ICP-MS. (b) Specifications of online elution device. (c) The ferrihydrite sample before and after online ICP-MS analysis. The eluents (1−5) are H_2O, NH_4NO_3, $NH_4H_2PO_4$, ammonium oxalate, and HF/HNO_3, respectively.

species associated with ferrihydrite including nonspecifically adsorbed, specifically adsorbed, iron oxide bonded, and residual species were successively extracted and detected by selecting appropriate eluents. The method enabled fractionation analysis of As species adsorbed onto the iron oxides without tedious sample pretreatment with high throughput and rich information.

EXPERIMENTAL SECTION

Preparation of As-Adsorbed Ferrihydrite Samples. Adsorption experiments were conducted in both a single system (only one species was present) and a binary system (As(III) and Sb(III) or As(V) and Sb(V)) under an initial pH of 6.5.[7,16] After adsorption reached equilibrium, the precipitates were collected as samples for further analysis. The detailed description of the adsorption experiment could be found in the Supporting Information (SI). The XRD pattern showed that synthesized ferrihydrite displayed two broad asymmetrical peaks located at 2θ of 35 and 62°, respectively (Figure S1), indicating formation of amorphous iron (oxy)-hydroxide (PDF#29-0712). The surface area of the obtained ferrihydrite was about 125 m^2 g^{-1}. The XPS analysis of the precipitate after adsorption showed that As was efficiently adsorbed by ferrihydrite, since an As 2p peak at 1327 eV, As 3p peak at 147 eV, and As 3d peak at 46 eV were all detected (Figure S2).

Online Sequential Analysis by ICP-MS. Online sequential detection of As species adsorbed onto the surface of ferrihydrite was carried out using a commercial ICP-MS (iCAP RQ, Thermo Fisher Scientific) equipped with a homemade online sequential elution device (Figure 1), which was easily fabricated by inserting a 100 μL micropipette tip (the upper part with the big opening was cut off) into another. A small portion of glass wool (ca. 10 mm^3) was fitted into the tip of elution device to avoid any intrusion of fine particles. Solid sample (about 1.0 mg) was laid on the glass wool. The elution device had a small dead volume (ca. 30 μL), which ensured a high extraction efficiency of analytes. Since the flow rate of eluents was 800 μL/min, the dead time was about 2.3 s. H_2O, NH_4NO_3, $NH_4H_2PO_4$, ammonium oxalate, and HF/HNO_3 were used as eluents, which displayed different degrees of interaction with various As fractions, showing a high

selectivity (SI). The extraction process was assisted with ultrasonication and heating (e.g., 120 W, 60 °C). Extracted analytes were then mixed with 2% HNO_3 through a Y connector (0.5 mm PEEK, Thermo Fisher Scientific) and subsequently transported to the injection system of ICP-MS. When a certain As fraction was completely extracted (indicated by generation of a complete peak), another eluent was utilized for elution of a different As species. For this, the sampling tube was taken out of the eluent and immediately inserted into the next eluent to avoid the introduction of air bubbles, which may lead to signal fluctuation.

RESULTS AND DISCUSSION

Correlation of As and Fe during Sequential Online Analysis. Figure 2 showed the online detection of As(III) and
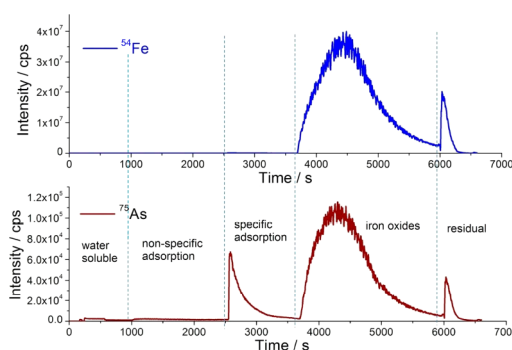

Figure 2. Sequential detection of As(III) (^{75}As) adsorbed onto ferrihydrite as well as the corresponding changes of ^{54}Fe.

the corresponding changes of Fe (^{54}Fe). It can be seen that different As peaks were generated as a function of elution time, indicating that various As species of water-soluble, nonspecifically adsorbed, specifically adsorbed, iron oxide bonded, and residual components were efficiently extracted by H_2O, NH_4NO_3 (5%),[17] $NH_4H_2PO_4$ (0.2 M),[18,19] ammonium oxalate (0.1 M, pH = 3),[17] and HF (0.5% mixed with 5% HNO_3),[20] respectively. The largest peak for As (extracted by ammonium oxalate) revealed that As(III) adsorbed onto ferrihydrite mainly exist as iron oxide bonded species (83%). Specifically adsorbed species (extracted by $NH_4H_2PO_4$) also accounted for a substantial amount (13%). The peak of a residual species (4%) indicated that a small amount of As was firmly confined inside the crystal structure, which was probably formed initially via coprecipitation or incorporation by ferrihydrite particles and subsequently embedded into the iron oxide structures.[21] In comparison, neither water-soluble nor nonspecifically adsorbed species were detected. The results indicated that As(III) could be strongly stabilized by ferrihydrite.[22]

On the other hand, a close correlation between As and Fe was observed, since two ^{54}Fe peaks were also detected along with ^{75}As. It is worth noting that when the fraction of specifically adsorbed As(III) was efficiently extracted by $NH_4H_2PO_4$, no Fe was detected indeed (Figure 2), which was probably due to the fact that this part of As(III) was specifically adsorbed by ferrihydrite via the formation of surface complexations[22] and could be efficiently displaced by PO_4^{3-}. In fact, P and As have similar electron configurations; however, the smaller size and higher charge density of PO_4^{3-} enabled it to outcompete As for adsorption sites.[23,24] With the

increase of elution time, the precipitate was gradually dissolved by ammonium oxalate and HF respectively, and therefore, Fe and As were released simultaneously. After being eluted by the HF/HNO$_3$ mixture, the precipitate eventually disappeared (Figures 1(c) and 2), leading to a complete release of Fe and preadsorbed As(III).

Online Detection of As(III) and As(V). In order to better understand the behavior of As on the surface of ferrihydrite, competitive ions of Sb were added. Figure 3 showed the
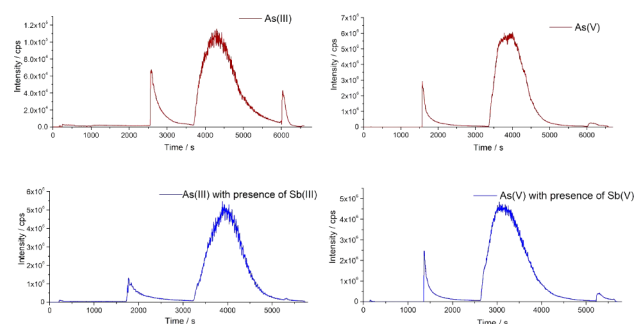

Figure 3. Sequential online detection of As(III) and As(V) in single and binary systems (As(III) + Sb(III) or As(V) + Sb(V)).

sequential online detection of As(III) and As(V) in a single system and binary system (As(III) + Sb(III) or As(V) + Sb(V)) (the behavior of Sb is shown in Figure S3). Generally, As(III) and As(V) both dominantly existed in the iron oxide bonded form, indicated by the largest peak. The fraction of specifically adsorbed As (the first peak) was also detected in the four analyses, indicating the formation of surface complexations on iron oxides.[25]

On the other hand, As(III) in a single system showed a slightly higher proportion of specifically adsorbed As than As(III) with the presence of Sb(III), probably due to the fact that As(III) and Sb(III) would compete for limited specific adsorption sites in a binary system.[16] As for As(V), it behaved more or less the same with or without the presence of Sb(V), as evidenced by a previous study about the coadsorption of As(V) and Sb(V) under competitive conditions[7] that showed that the presence of Sb(V) only had a minor effect on As(V) adsorption in a coexisting system. The online detection of As(III) and As(V) in either a single or binary system suggested that though As(III) and As(V) performed similarly on chromatographic performance, the differences of peak area and intensity could be used to evaluate their adsorption behaviors.

Quantitative Online Sequential Analysis of As. In order to quantify different fractions of As by online ICP-MS analysis, the limit of detection (LOD) and linearity of As(III) and As(V) were also evaluated. The detection limit was calculated according to the recommendation of the IUPAC (International Union of Pure and Applied Chemistry) as the corresponding concentration of 3 times the standard deviation for the signal/noise (S/N) ratio for each species. The obtained detection limits for As(III) and As(V) were 0.008 and 0.013 μg/kg. The calibration curves were plotted based on integrated area as a function of absolute mass weight. Specifically, 200 μL aliquots of different concentrations of As standards (10, 20, 50, 100, 1000 μg/L, respectively) were sequentially injected into the online analysis system, generating a series of peaks with different areas and heights (Figure S4). The result showed that

the integrated peak area was linearly correlated with the mass weight of analytes, with the correlation coefficient close to 1 for both As(III) and As(V). Therefore, peak areas were used for quantitative analysis of analytes. A spike recovery experiment was also conducted by adding 200 μL of 10 mg L^{-1} As standard (2 μg) to As-preadsorbed ferrihydrite samples, which were then analyzed by online sequential analysis (Figure S5). The obtained spike recovery ranged from 90 to 110%, with the relative standard deviation (RSD) less than 10% (Table S1).

As Fractionation on the Surface of Ferrihydrite. The aqueous phase after the adsorption experiment and the obtained precipitate were analyzed respectively for mass balance calculation (see SI). Then, based on the weight of precipitate and the quantitative analysis, each fraction of As species was calculated. First of all, As(III) showed a stronger adsorption than As(V) in both single and binary systems (9.10 vs 8.16 mg/L in a single system and 8.67 vs 7.79 mg/L in a binary system) (Table S2), indicating that As(III) would be preferentially stabilized by iron oxides as opposed to As(V). In addition, both As(III) and As(V) in a single system demonstrated a higher adsorption than in a binary system (9.10 and 8.16 mg/L in a single system vs 8.67 and 7.79 mg/L in a binary system) due to their competition for adsorption sites. The proportion of specifically adsorbed As(III) was 13%, higher than that of As(III)-binary (9%) (Figure 4, Table S3).
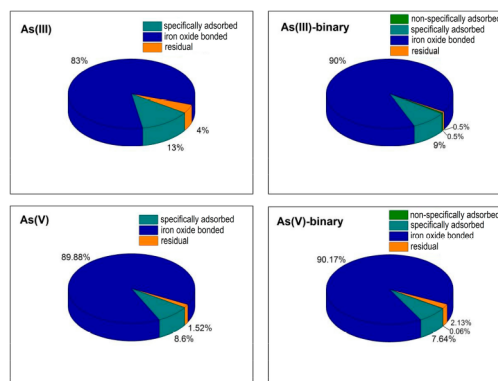

Figure 4. Distribution of various fractions of As (specifically adsorbed, nonspecifically adsorbed, iron oxide bonded, and residual) adsorbed onto ferrihydrite.

The proportion of iron oxide bonded As(III) (83%), however, was lower than that in a binary system (90%). On the other hand, the fractionation of As(V) in either a single or binary system was highly similar to As(III), with about 90% of As(V) associated with iron oxide and around 8% for specific adsorption. Clearly, unlike conventional analytical methods, sequential online analysis by ICP-MS could provide more information with respect to As fractionation and its association with iron oxides (Figure S6).

Validation of the Method. The developed method was also validated with a conventional analytical procedure[26] and analysis of real soil samples (Table S4). Generally, different As fractions obtained from online sequential analysis were in good agreement with that of conventional offline extraction (Table S5 and Figure 5), with iron oxide bonded species as the main existing form (85−90%). However, the overall analysis time for the approach was less than 2 h, with comparison of more than 24 h for conventional treatment. In addition, a reference soil sample (GBW07404) was analyzed. As a result, the detected
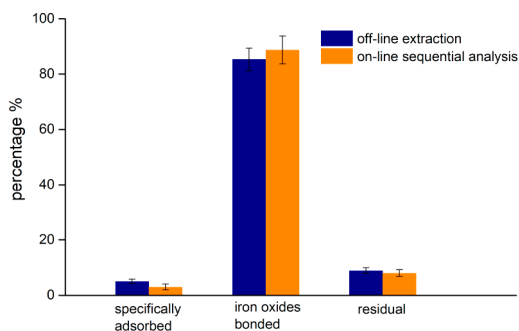
Figure 5. As fractions determined by online sequential ICP-MS analysis and conventional extraction procedures.

concentration (52 ± 3 μg/g) was in good agreement with the certified value (58 ± 6 μg/g), with an RSD of 5.1% and spike recovery of 90% (Table S4). The results demonstrated that the method could be practically used for direct analysis of solid samples.

CONCLUSIONS

Online sequential fractionation analysis of As adsorbed onto the surface of iron oxides was proven to be a useful tool for studying its geochemical behaviors, such as toxicity and mobility. For instance, exchangeable As on the surface of adsorbents may lead to a high toxicity level in an aquatic environment. Meanwhile, the fraction of As associated with iron oxides indicated a strong stability. The developed method features extremely low sample consumption and minimized sample pretreatment. It is worth noting that considering the matrix complexity of real samples, the elution conditions such as the components of eluents, elution time, and applied energy may need to be optimized to reduce the matrix influence and improve the extraction efficiency of various analytes. The approach may find its potential applications in different fields, such as the structural characterization of solid materials, fraction analysis of rare earth elements, adsorption mechanism study of metal elements, and contamination prediction of toxic elements in an aquatic environment.

ASSOCIATED CONTENT

Supporting Information

The Supporting Information is available free of charge at https://pubs.acs.org/doi/10.1021/acs.analchem.0c03516.

Reagents and apparatus; preparation of ferrihydrite samples; mass balance calculation; XRD and XPS pattern of ferrihydrite; sequential online detection of Sb; calibration curve and spike recovery; analysis of soil samples; data for aqueous phase, precipitate, spike, As species distribution; and conventional extraction conditions (PDF)

AUTHOR INFORMATION

Corresponding Author

Huanwen Chen − *Jiangxi Key Laboratory for Mass Spectrometry and Instrumentation, East China University of Technology, 330013 Nanchang, P. R. China;* Email: chw8868@gmail.com; Fax: (+86)791-83896370

Authors

Debo Wu − *Jiangxi Key Laboratory for Mass Spectrometry and Instrumentation, East China University of Technology, 330013 Nanchang, P. R. China;* ⊙ orcid.org/0000-0002-3209-406X

Shuiping Yang − *Jiangxi Key Laboratory for Mass Spectrometry and Instrumentation, East China University of Technology, 330013 Nanchang, P. R. China*

Faliang Li − *Jiangxi Key Laboratory for Mass Spectrometry and Instrumentation, East China University of Technology, 330013 Nanchang, P. R. China*

Tenggao Zhu − *Jiangxi Key Laboratory for Mass Spectrometry and Instrumentation, East China University of Technology, 330013 Nanchang, P. R. China*

Complete contact information is available at:
https://pubs.acs.org/10.1021/acs.analchem.0c03516

Author Contributions

The manuscript was written through contributions of all authors.

Notes

The authors declare no competing financial interest.

REFERENCES

(1) Okkenhaug, G.; Zhu, Y.-G.; He, J.; Li, X.; Luo, L.; Mulder, J. *Environ. Sci. Technol.* **2012**, *46* (6), 3155−3162.

(2) Fu, Z.; Wu, F.; Amarasiriwardena, D.; Mo, C.; Liu, B.; Zhu, J.; Deng, Q.; Liao, H. *Sci. Total Environ.* **2010**, *408* (16), 3403−3410.

(3) Huang, J. H.; Kretzschmar, R. *Anal. Chem.* **2010**, *82* (13), 5534−5540.

(4) Keon, N. E.; Swartz, C. H.; Brabander, D. J.; Harvey, C.; Hemond, H. F. *Environ. Sci. Technol.* **2001**, *35* (13), 2778−2784.

(5) Voegelin, A.; Weber, F.-A.; Kretzschmar, R. *Geochim. Cosmochim. Acta* **2007**, *71* (23), 5804−5820.

(6) Javed, M. B.; Kachanoski, G.; Siddique, T. *Anal. Chim. Acta* **2013**, *787*, 102−110.

(7) Wu, D.; Sun, S.; He, M.; Wu, Z.; Xiao, J.; Chen, X. D.; Wu, W. D. *Environ. Sci. Pollut. Res.* **2018**, *25*, 14585.

(8) Wu, D.; Pichler, T. *Geochem.: Explor., Environ., Anal.* **2016**, *16* (2), 117−125.

(9) Quevauviller, P.; Rauret, G.; Muntau, H.; Ure, A. M.; Rubio, R.; López-Sánchez, J. F.; Fiedler, H. D.; Griepink, B. *Fresenius' J. Anal. Chem.* **1994**, *349* (12), 808−814.

(10) Tessier, A.; Campbell, P. G. C.; Bisson, M. *Anal. Chem.* **1979**, *51* (7), 844−851.

(11) Wu, D.; Sun, S. *Trends Environ. Anal. Chem.* **2016**, *11*, 9−22.

(12) Breuer, C.; Pichler, T. *Chem. Geol.* **2013**, *348*, 2−14.

(13) Kersten, M.; Karabacheva, S.; Vlasova, N.; Branscheid, R.; Schurk, K.; Stanjek, H. *Colloids Surf., A* **2014**, *448*, 73−80.

(14) McComb, K. A.; Craw, D.; McQuillan, A. J. *Langmuir* **2007**, *23* (24), 12125−12130.

(15) Dong, L. M.; Yan, X. P. *Talanta* **2005**, *65* (3), 627−631.

(16) Qi, P.; Pichler, T. *J. Hazard. Mater.* **2017**, *330*, 142−148.

(17) Johnston, S. E.; Barnard, W. M. *Soil Sci. Soc. Am. J.* **1979**, *43*, 304−308.

(18) Wenzel, W. W.; Kirchbaumer, N.; Prohaska, T.; Stingeder, G.; Lombi, E.; Adriano, D. C. *Anal. Chim. Acta* **2001**, *436* (2), 309−323.

(19) Georgiadis, M.; Cai, Y.; Solo-Gabriele, H. M. *Environ. Pollut.* **2006**, *141* (1), 22−29.

(20) Keon, N. E.; Swartz, C. H.; Brabander, D. J.; Harvey, C.; Hemond, H. F. *Environ. Sci. Technol.* **2001**, *35* (13), 2778−2784.

(21) Jia, Y.; Xu, L.; Fang, Z.; Demopoulos, G. P. *Environ. Sci. Technol.* **2006**, *40* (10), 3248−3253.

(22) Qi, P.; Pichler, T. *Langmuir* **2014**, *30* (37), 11110−11116.

(23) Niazi, N. K.; Burton, E. D. *Environ. Pollut.* **2016**, *218*, 111−117.

(24) Arco-Lázaro, E.; Agudo, I.; Clemente, R.; Bernal, M. P. *Environ. Pollut.* **2016**, *216*, 71−79.

(25) Ma, J.; Guo, H.; Lei, M.; Zhou, X.; Li, F.; Yu, T.; Wei, R.; Zhang, H.; Zhang, X.; Wu, Y. *Water, Air, Soil Pollut.* **2015**, *226* (8), 260.

(26) Drahota, P.; Grösslová, Z.; Kindlová, H. *Anal. Chim. Acta* **2014**, *839*, 34−43.